encit 2020

ABCM Associação Brasileira de Engenharia e Ciências Mecânicas

18th Brazilian Congress of Thermal Sciences and Engineering
November 16-20, 2020 (Online)

ENC-2020-0713
AN ALGORITHMIC APPROACH FOR COUPLING CREEP INDUCED STRAIN AND ANNULAR PRESSURE BUILDUP IN OIL WELLS

Eduardo B.D.M. Alves
Arthur P. da Veiga
Eduardo A. Fancello
Jader R. Barbosa Jr.
Departamento de Engenharia Mecânica, Universidade Federal de Santa Catarina, Florianópolis, SC, 88040-900, Brazil
eduardo.alves@polo.ufsc.br
arthur.veiga@polo.ufsc.br
eduardo.fancello@ufsc.br
jrb@polo.ufsc.br

Abstract. *This paper presents a new algorithmic formulation to couple a state-of-the-art thermal solver, used for computing Annular Pressure Buildup in deep sea oil producing wells, with a novel procedure for calculating creep behavior in salt layers. The latter makes use of a basic non linear solid model based on a constitutive relationship developed for salt rocks. The thermal model solves momentum and energy balance equations (coupled with radial thermal resistances for the concentric wellbore regions) to determine the pressure and temperature on the production fluid. The results, which are discussed in the light of qualitative and quantitative comparisons using a real well geometry, look promising, therefore indicating the validity of the new approach. Moreover, a direct relation between APB and the creep amplitude was identified for the case tested. The model seems to confirm that the effects of creep are not significant for the initial lifespan of wells.*

Keywords: *APB, Creep, Salt Simulation, FEM*

1. INTRODUCTION

In the context of oil producing wells, the Brazilian Pre-Salt cluster is receiving considerable attention due to its potential and production capacity. However, in order to fulfill this potential, many technical difficulties need to be addressed. Over the years, a recurring challenge is related to drilling through the salt layer (Poiate Jr. *et al.*, 2006), and many associated factors, such as wellbore instability, casing damage and salt creep (Zhang *et al.*, 2008).

Jaeger *et al.* (2007) defines creep as the continuous strain related to a given constant load. It can usually be separated in three main stages, namely the transient flow, the steady-state flow and the tertiary creep. Transient flow can be characterized by a high creep rate which slows down until steady-state is reached. Here, as long as the stress is kept constant, the creep rate remains constant. If this condition remains for a long period of time, then it is possible for the creep rate to increase once again due to damage in the material; this period of late acceleration is called tertiary creep. Generally, for oil producing wells, the steady state is the most relevant stage, since transient flow settles quickly after perforation and completion of the well. Also, any damage in the rock formation is contained by the casings and cementation, so tertiary creep usually is not considered (Wang and Samuel, 2016).

In the long term, after drilling is completed, and during the producing life of the well, salt creep related issues may occur, as indicated by de Almeida (2016). Taheri *et al.* (2020) points to a reduction of design safety factors if the salt layer creep behavior is taken in account.

Salt creep may occur in conjunction with and have some influence on the already well documented phenomenon of Annular Pressure Buildup (APB), which is a consequence of the thermally driven expansion of the fluids present in the concentric annuli (Oudeman and Bacarreza, 1995). The heat source, in this case, is the production fluid, and the consequences of the annulus pressure increase can lead to catastrophic events, such as those which took place during the perforation of a well in the Gulf of Mexico, where a collapsed casing trapped the drill-string during the perforation (Pattillo *et al.*, 2006). Fig. 1 shows the collapsed casing of a well, attributed to APB. In the more specific case of wells surrounded by salt formations, the creep related displacement can contribute to APB, since the total volume of the annular space may vary with time.

Figure 1: Collapsed casing (Pattillo *et al.*, 2006).

In general, salt layers can either close or open around the well, acting both towards reducing or increasing the pressure. de Almeida (2016) presented a calculation procedure in which two different commercial software packages for thermal simulation of petroleum wells and mechanical/structural simulation were combined to predict the influence of thermal phenomena in the salt creep behavior. However, since the simulations were performed in completely separated programs, the process of integrating the results had to be performed externally through Python scripts. This forced the approach for computing APB to be approximated by means of virtual mass injections in the annulus which is not ideal since for most cases there are no leaks or mass increase in this regions.

This paper proposes a new coupling technique between a mechanical model to solve the viscoelastic behavior of the salt layer and the thermal model to compute the property dependent temperature profiles in the wellbore geometry. By solving the equations in a single routine the coupling process is more dynamic and both systems can interact with each other directly. So it is possible to use a more robust approach, based on the conservation equations, in order to solve the problem.

2. METHODOLOGY

In order to model the APB in oil producing wells this paper tackles the problem in three different stages. First it proposes a numerical approach to solve creep related deformations in salt layers. Next, a brief overview of an existing model for predicting APB due to heat transfer in producing wells is presented. Lastly, the coupling scheme for solving APB with creep induced deformation in the annulus is discussed in detail.

2.1 Salt Layer Displacement Model

In order to model the deformation resulting from creep in salt layers, it is first necessary to understand the stress condition to which the material will be subjected. This stress condition can be known using methodologies similar to those presented in Fjaer *et al.* (2008).

To determine the vertical stress condition to which the salt column will be subjected, the formation overburden gradient will be used. When doing this the overload voltage can be written by:

$$\sigma_{ov} = 1174.74 G_{ov} Z \tag{1}$$

Since the overburden gradient is known at discrete depths it is possible to use linear interpolation to determine the value of the vertical stress applied in the salt layer. It is important to emphasise that Z is the vertical depth, this being the vertical distance to the sea level.

Also, once known the vertical stress, it is possible to estimate the complete initial stress state of the rock. Many authors points on how to do this estimation, the basic idea used for the models in this paper are derived based on the models used in de Almeida (2016). First, in order to determine the initial stress it is considered pure elastic deformation such that, for far distances from the well the displacement is null in the radial direction. Also the upper boundary condition will be the constant load derived from the overburden gradient, meanwhile the lower boundary condition will consider that there will be no displacement in the vertical direction. The inner boundary condition, the model will consider the pressure due to the hydrostatic pressure from the drilling mud.

This set of boundary conditions can be applied to model the initial state of displacement and stress, however, for the reaming lifespan of the production well it is necessary to model the displacement behavior in conjunction with the stress. As previously mentioned, the creep phenomenon can be simulated using classical incremental formulations for viscoelastic / viscoplastic materials (see, for example, de Souza Neto *et al.* (2008), Mendonça and Fancello (2019) or Naumenko (2006)). Most of these formulations seek for the displacement field $\boldsymbol{u}(x,t)$ of the deformable body that, due

to an appropriate constitutive equation, produces a stress field which is in mechanical balance with the external forces at any time.

The model used in the present work is summarized in Eqs. (2-5). Assuming linear kinematics, the total strain tensor $\boldsymbol{\varepsilon}$ at each material point x and time t is additively decomposed in elastic $\boldsymbol{\varepsilon}_{el}$ and plastic $\boldsymbol{\varepsilon}_{cr}$ contributions Eq. 2. The stress is then calculated as a linear isotropic function of the elastic strain state Eq. 3 while the creep strain evolves in time as a function of the stress state. In equation Eq. 4 the scalar $\dot{\gamma}$ denotes the amplitude of the strain rate while the the isochoric tensor $\boldsymbol{N}$ defines the direction of the creep flow . The expression for the rate $\dot{\gamma}$ is a key point in present approach and follows the creep law shown in Poiate Jr. *et al.* (2006). This law assumes that the creep strain rate is directly dependant on the effective stress $\boldsymbol{\sigma}_{eff}$. In this work this stress is calculated using the equivalent von-Mises operation over the stress tensor $\boldsymbol{\sigma}$, similarly to what was used in de Almeida (2016).

$$\boldsymbol{\varepsilon} = \boldsymbol{\varepsilon}_{el} + \boldsymbol{\varepsilon}_{cr} \tag{2}$$

$$\boldsymbol{\sigma} = \mathcal{C}\boldsymbol{\varepsilon}_{el} = \mathcal{C}\left(\boldsymbol{\varepsilon} - \boldsymbol{\varepsilon}_{cr}\right) \tag{3}$$

$$\dot{\boldsymbol{\varepsilon}}_{cr} = \dot{\gamma}\boldsymbol{N}\left(\boldsymbol{\sigma}\right) \tag{4}$$

$$\dot{\gamma} = \begin{cases} \dot{\gamma}_0 \left(\frac{\sigma_{eff}}{\sigma_0}\right)^{n1} \exp\left(\frac{Q}{RT_0} - \frac{Q}{RT}\right), & \text{if } \sigma_{eff} < \sigma_0 \\ \dot{\gamma}_0 \left(\frac{\sigma_{eff}}{\sigma_0}\right)^{n2} \exp\left(\frac{Q}{RT_0} - \frac{Q}{RT}\right), & \text{otherwise} \end{cases} \tag{5}$$

In Eq.5, $\dot{\gamma}_0$ and σ_0 denote the reference creep rate and tension, respectively. Q is the activation energy of the creep flow, R is the universal gas constant, T_0 is the reference temperature at which the creep calibration tests occurred. Finally, n_1 and n_2 are empirical constants. Equation 5 was calibrated using real Pre Salt saline rocks such as Halite, Carnalite and Tachyhydrite, this calibration can be found in Poiate Jr. *et al.* (2006).

Equation 5 is known as rate constitutive equations and in order to evolve in time a numerical integration scheme is needed. A classic choice for these kind of equations is the fully implicit Euler procedure. Time is divided in finite time increments $\Delta t = t_{n+1} - t_n$. The incremental approximation of Eq. 4 takes the form (de Souza Neto *et al.*, 2008):

$$\Delta\gamma = \Delta t\dot{\gamma}_{n+1} \tag{6}$$

$$\boldsymbol{\varepsilon}_{cr,n+1} = \boldsymbol{\varepsilon}_{cr,n} + \Delta\gamma\boldsymbol{N}_{n+1} \tag{7}$$

The subindex $n+1$ in Eq. 6 indicates that Eq. 5 is calculated using the stress state at the end of the time increment (implicit scheme). Equation 7 shows the rule to update the creep strain state. This implicit scheme drives then to a coupled system of algeabric equations that is solved using Newton method within a procedure kown in the literature as Predictor-corrector algorithm. When solved, the updated stress and strain states at the end of the time increment are finally known.

The updated stress field state is meant to be in balance with the external forces. Balance equations are stated by the principle of virtual power and its approximate solution is obtained here using the finite element method. Equation 8 shows the expression of the so called residual force vector which is a nonlinear function of the nodal displacement $\boldsymbol{U}_{n+1}$ of the FE mesh at the end of the time increment. The first term at the r.h. is the internal force given by a volume integration of the updated stresses. $\boldsymbol{B}$ is a matrix containing the derivative of the shape FE functions. Second and third terms represent the external force vector, given by volume and surface integration of the external forces $\boldsymbol{b}$ and $\boldsymbol{t}_{n+1}$ respectively. Matrix $\mathcal{N}$ contains the value of the shape functions over the FE mesh.

$$Res\left(\boldsymbol{U}_{n+1}\right) = \int_{\Omega} \boldsymbol{B}^T \sigma_{n+1} \boldsymbol{B} d\Omega - \int_{\Omega} \mathcal{N}^T \boldsymbol{b} d\Omega - \int_{\partial\Omega} \mathcal{N}^T \boldsymbol{t}_{n+1} d\partial\Omega \tag{8}$$

The surface forces t_{n+1} depend on the given boundary conditions while the body forces $\boldsymbol{b}$ represent the weight of the salt layer and come from the derivative of Eq. 1 with respect to depth.

With this residual sets of equations it is possible to solve a non linear problem to find the sets of nodal displacements which would grant mechanical balance for the material. This non linear problem is solved via Newton method, with the derivatives of the residual functions taken analytically.

Taking advantage of the axial symmetry of the problem, an axial simmetric finite element formulation is used, reducing the numerical problem to a 2D fields. Biquadratic Lagrangian finite elements with 3 x 3 gauss integration points were used for the computations. Figure 2 shows schematically a discretization with 6 elements with applied boundary conditions.

The figure shows the pressure in the exposed annulus. This variable is taken directly from the thermal solver, being the variable which couples the two systems (wellbore and formation).

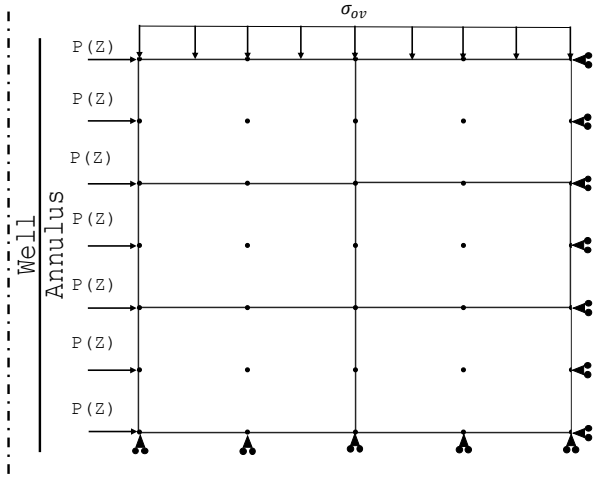

Figure 2: Boundary conditions used for the simulation

2.2 Thermal Solver

To resolve the thermal phenomena and compute their contribution to the annular pressure, the present study adopts the formulation presented in da Veiga *et al.* (2020). This model, in turn, was built upon previous works on the same subject Barcelos (2017).

The thermal solver considers that the heat transfer within the well evolves in a pseudo steady state, where the thermal capacities of the annuli and production fluid are neglected, and the formation is treated as a semi-infinite solid. This approach is similar to that of Hasan and Kabir (2012), where the heat transfer is predicted using equivalent thermal resistances from the production fluid to the formation wall. The temperature of the interface between the wellbore and the formation is traditionally simulated using the so-called time functions, which are essentially approximations of analytical solutions of the constant heat flux conditions to the formation, solved with Laplace transforms (Hasan and Kabir, 1991). In this work, Laplace transforms were used to determine the temperature distribution in the formation, using an inverse transform algorithm to find the time equivalent solution; the Stehfest algorithm was chosen due to its good accuracy with exponential like problems (Kuhlman, 2013).

To solve the energy and momentum balance equations for the production fluid, 4^{th}-order Runge-Kutta method was employed. The pressure distributions in the fluids trapped in the annuli were obtained from a procedure which involves integrating the hydrostatic equation with a boundary condition which satisfies the mass conservation.

The procedure for obtaining a converged solution consists of applying the mass conservation in every annuli and solving numerically the mass balance considering local density variations due to thermal expansion of the annular fluid. Convergence is achieved when the annular mass in the end of any given time step is equal to the mass in place at the initial condition of the well.

In most works, the APB is computed as a single value for the entire annulus volume. da Veiga *et al.* (2020) presents a formulation where APB is a result of the local diference from the final pressure and the initial pressure at every depth, resulting in a APB profile inside the annulus. For this work APB is defined as the maximum value that the profile can have in the annulus.

2.3 Coupling Between the Well Thermal Solver and the Creep Model

The coupling algorithm takes advantage of the above mentioned mass conservation iteration loop implemented on the thermal solver. Basically, it incorporates the displacements calculated in the salt module into the mass conservation procedure, by changing the effective cross-section area of the annulus. Since the iterative procedure already seeks the correct pressurization to satisfy the mass conservation, both models are solved using the same set of convergence parameters and variables of interest.

3. TEST AND PRELIMINARY RESULTS

To test the novel approach proposed here for coupling both models, we use a standard geometry with a formation layer exposed to the annular space. The analysis consists of evaluating the results with and without the salt creep model activated. Therefore, it will be possible to qualitatively (and quantitatively) assess the influence of the salt layer on the behavior of the annular pressure and, therefore, judge if the coupling algorithm returns a physically consistent behavior.

The well geometry considered in this simulation is the same as the one previously studied by Barcelos (2017). Tables

1 and 2 present the well geometry in detail.

Table 1: Geometric parameters for casings and cementing

Tubular Name	OD [m]	MD [m]			Hole Size [m]	Fluid Density [$\mathrm{kg\,m^{-3}}$]
		Tub. top	Cement top	Tub. base		
Casing 1	0.762	1109.5	1109.5	1170.0	0.914	-
Casing 2	0.508	1109.5	1109.5	1909.0	0.660	-
Casing 3	0.339	1109.5	1802.0	3543.0	0.406	1138.0
Casing 4	0.244	1109.5	4050.0	4935.0	0.311	1138.0
Prod Tubing	0.139	1109.5	-	4250.0	-	1150.0

Table 2: Lithology

Formation	MD [m]	
	Top	Base
Shale	1110.0	1902.7
Marl	1902.7	2310.7
Shale	2310.7	2672.3
Sandstone	2672.3	2689.3
Shale	2689.3	2785.3
Calcilutite	2785.3	2836.9
Shale	2836.9	3481.4
Marl	3481.4	3689.8
Calcilutite	3689.8	4119.5
Shale	4119.5	4297.0
Wackestone	4297.0	4320.0

Figure 3 presents an axisymmetric cutaway view of the wellbore, with a color scheme to differentiate between the different materials. The figure is in scale in relation to the depth axis, however it is not in scale with respect to the radius of the well.

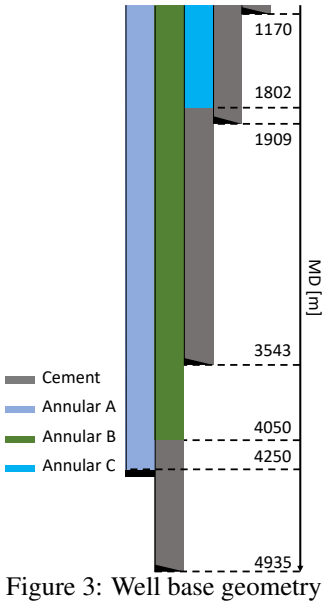

Figure 3: Well base geometry

It is important to emphasise that, in the original wellbore geometry there was no salt layer in contact with the annular space. In other words, we have deliberately added the creep behavior using Halite properties to the Marl layer to simulate the creep behavior in the well. The test layer is located at depths between 3481.4 m and 3689.8 m. Also, in the original well, this region has a certain degree of inclination from the vertical but, since the structural model was developed only to deal with vertical wellbores, we are also neglecting the inclination effects in this preliminary evaluation of the solver.

Another input variable for the model, since it is unknown variable for the original well, it was also added an theoretical

overburden gradient. For the region of interest it can be calculated by the linear interpolation from the closest points provided. For the scenario simulated a value of 13.8 $\mathrm{lbm\,gal^{-1}}$ at 3000 m, and 18.9 $\mathrm{lbm\,gal^{-1}}$ at 4573.74 m.

An important factor to be considered is whether the Marl layer will deform away from the center line or it will reduce the annular space. In order to predict this behavior, one can use the same considerations as Fjaer *et al.* (2008) who related vertical stress and horizontal stress in a lithostatic state using the Poisson coefficient given by:

$$\sigma_h = \frac{\nu}{1-\nu}\sigma_{ov} \tag{9}$$

When checking the *in-situ* behavior during the simulation, Eq. 9 indicates that the pressure in the annulus is greater than the horizontal component of the lithostatic tension along the entire layer. Thus, it is expected for the displacement to cause the inner formation radius to move away from the well. This should increase the volume of the annulus resulting in a reduction of the APB by the end of the simulation.

The basic discretization of the structural grid consisted of 300 elements, with 30 elements in the radial direction and 10 in the axial direction. For the time domain, a brief convergence test was performed using the final APB result, reaching a discretization with a smaller spacing in the first year and a geometric spacing starting at the end of the first year until the end of of a period of 30 years.

In order to set the initial condition of the well, one needs to determine the initial temperature of the entire domain and the initial pressure in the annuli. For that, two assumptions are made. The first one is that the annuli and the production fluid are in thermal equilibrium with the formation, and the temperature, know for the entire well, depends on the well depth. Also, the fluids trapped in the annuli are assumed t be stagnated, so they must follow a hydrostatic profile. Since the fluids properties can be calculated from thermodynamic libraries, it is possible to set profiles of pressure and temperature pairs for each annulus, depending only on the temperature of the formation at each depth and the geometry of the well.

In the present well, the fluid filling annulus A is a saline base completion fluid. The fluids in the remaining annuli are oil based muds, which are modeled in a similar manner as Barcelos (2017). Also, in this well, a constant geothermal gradient of $0.027^{\circ}\mathrm{C\,m^{-1}}$ can be used to determine the initial temperature as a function of the depth.

The main results for a total production time of 30 years, namely the APB profile with and without the salt module activated, are presented in Fig. 4. From this, one can conclude that the main effect that dictates the behavior of the APB is the thermal component, as suggested by Oudeman and Bacarreza (1995). However, one can unequivocally argue that the salt creep (deformation) has a non-negligible contribution, which acts toward reducing the APB, as indicated above, from 17.48 MPa to 13.97 MPa when considering the effects of the salt layer.

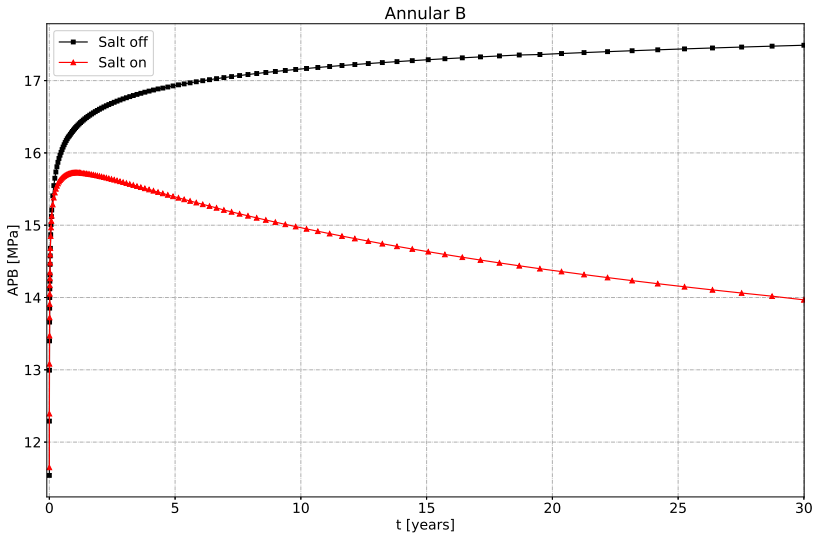

Figure 4: APB behavior in annular B with the salt creep model activated and not.

The above result is consistent with the physical behavior of the layer deformation. However when dealing with creep induced strain, another important variable in the validation process is the deviatoric tension. In this paper, this paremeter is computed using the Von Mises criterion and, in a natural creep induced strain, its magnitude must decrease during the deformation. Therefore, in Fig 5, comparisons of the Von Mises tension are presented for simulated times of 12 hours and after 30 years. It shows that the tension is indeed reduced along the production period of the well, which will result in a slower creep rate and progressively smaller displacements.

From these results, it is safe to assume that the behavior of both the structural model and the coupling algorithm point to a physically well behaved solution.

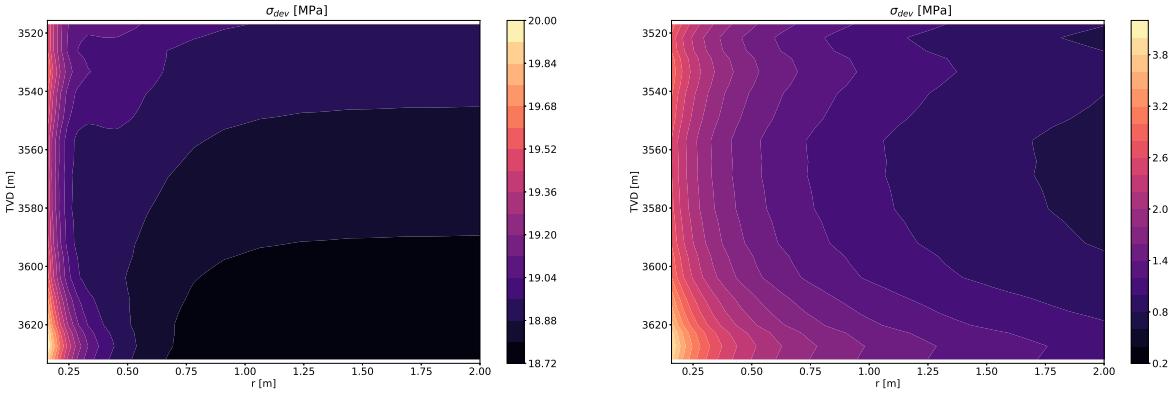

(a) Deviatoric stress in 12 hours (b) Deviatoric stress in 30 years

Figure 5: Transient behavior of deviatoric stress

This remark pertains to the behavior of the entire salt domain. However, it is also possible to use a single point in space to check for patterns and phenomena in the rock. For that, a "probe" is set at the position $r = 0.15848$ m and $MD = 3622.91$ m. This position is close to the wall and in the middle of the domain. There, it is possible to plot the profile of both the local deviatoric tension and the creep amplitude variable (γ). Fig. 6 presents the results from this probe.

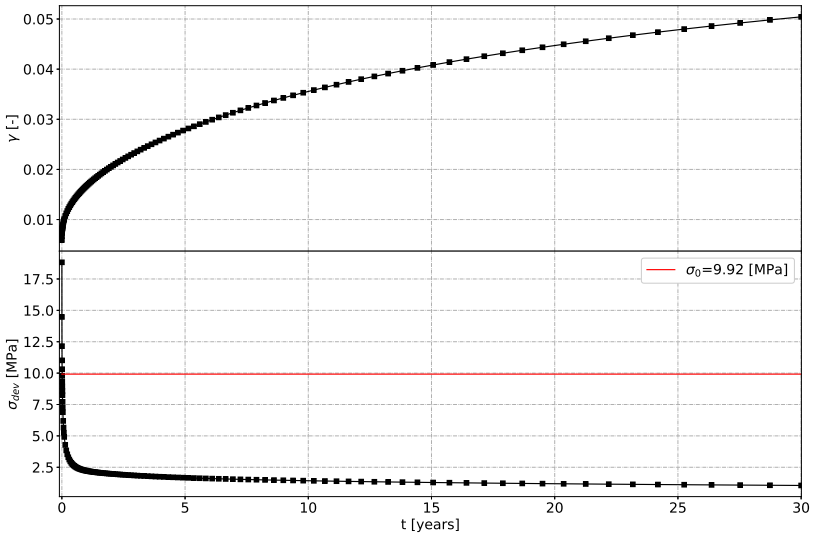

Figure 6: Integration node time profile for creep amplitude and deviatoric stress

Some important remarks can be made at this stage. First, it is clear that the temporal grid spacing used in the first year is not yet sufficient for the simulation. This is made clear by the discontinuities that exist during that period. However it is also possible to observe an extra important behavior in these results: even though the effective stress falls in a large steep in the first year, the creep amplitude continues to increase with a significant rate until the end of the simulation.

Another important remark is the close relation in the behavior of the APB, shown in Fig. 4, and the γ variable. At the beginning of the simulation, the APB is mainly governed by the thermal contribution, but as time progresses, the difference between the models (with salt creep and without) becomes similar to the behavior of this variable. Fig. 7 presents the difference in APB of both models isolated.

Figure 7 confirms the influence exerted by γ on the APB predicted by the model. This points to a variable which can be used to confirm the quality of the temporal discretization used in the simulation. Of course, γ is related to each point individually, so a complete analysis of all nodes is required to confirm this hypothesis. However, once performed, the observed behavior was similar to all remaining nodes.

All results presented so far refer mainly to the isolated behavior resulting from the presence of salt in the well. But it is also important to point out that the presence of salt could affect the heat transfer during production due to large displacements of the wellbore walls. Figure 8 presents the temperature profile in the production fluid inside the well after 30 years of continuous production. It shows that the effects in the temperature of the production fluid is small.

Also, up this point it is mentioned that the short transient of the production is mainly affected by the thermal com-

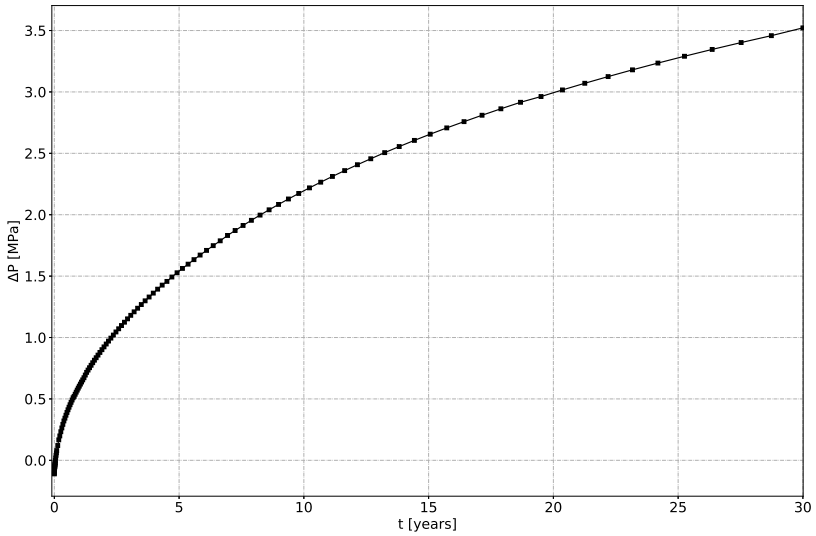

Figure 7: Difference in APB between the models with and without salt creep

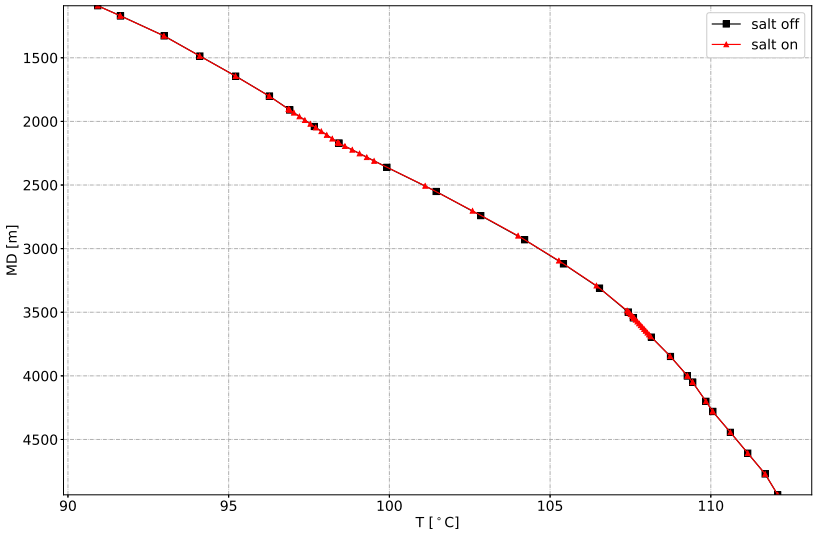

Figure 8: Temperature profile in production fluid after 30 years

ponent. This is mainly related to the fact that the temperature fluctuations are more noticeable in the firsts days of the production. To confirm this Fig. 9 presents the transient profile of the temperature in the wellhead for the entire simulation interval.

This confirms that the temperature in the wellhead settles quickly when compared to the behavior of the salt layer. From that, it is possible to conclude that the analysis of considering creep when simulating APB requires the simulation of long times, even reaching the entire lifespan of the well. For the short transient this phenomenon is of less importance.

As an combined analysis it is possible to affirm that as the temperature settles quickly, the increase of pressure in the annulus occurs quickly in the start of the production, and latter it is affected by the volume variation caused by the creep deformation.

4. Conclusion

Using a classical formulation for modeling the structural deformation on salt layers with creep behavior, this paper proposed a new algorithmic approach for coupling the thermal simulation in order to compute APB of oil producing wells. Preliminary results indicated that the model is physically consistent and qualitatively accurate. However, further tests are required to confirm the validity of this approach. Also, the results are useful to determine important variables to be used in following studies such as the creep amplitude, which is closely related to the APB behavior for long time simulations.

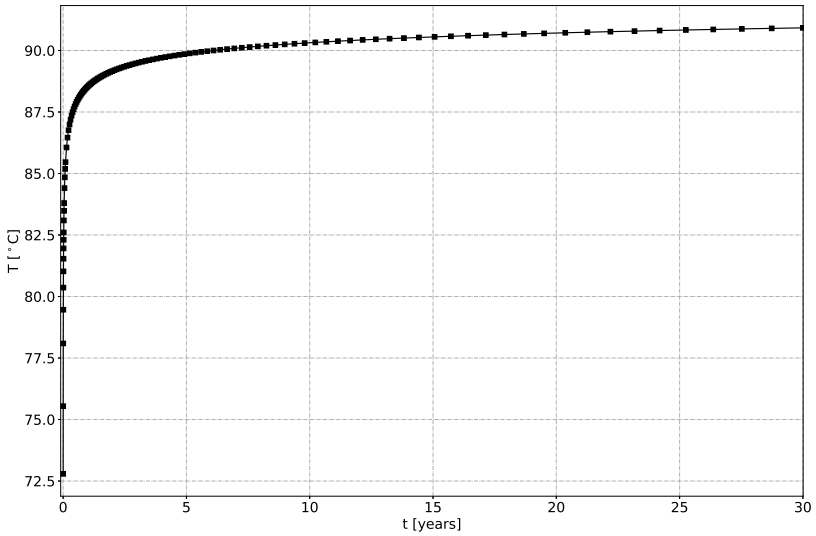

Figure 9: Temperature profile in the wellhead

5. ACKNOWLEDGEMENTS

The authors would like to acknowledge Capes for the financial support and Petrobras for both the financial support and for providing field data for the studies.

6. REFERENCES

Barcelos, J.G.A., 2017. *MODELAGEM MATEMÁTICA DO AUMENTO DE PRESSÃO NOS ANULARES (APB) EM POÇOS DE PETRÓLEO*. Ph.D. thesis, Universidade Federal de Santa Catarina.

da Veiga, A.P., Martins, I.O., Barcelos, J.G.A., Ferreira, M.V.D., Alves, E.B.D.M., da Silva, A.K. and Barbosa Jr., J.R., 2020. "Predicting Thermal Expansion Pressure Buildup in a Deep Offshore Well with an Annulus Partially Filled with Nitrogen Gas". In preparation for Journal of Petroleum Science and Engineering.

de Almeida, L.F.M., 2016. *Modelagem termo-mecânica do crescimento de pressão em anulares confinados , frente a formações salinas*. Dissertação, Pontifíca Universidade Católica do Rio de Janeiro.

de Souza Neto, E.A., Peri, D. and Owen, D.R.J., 2008. *Computational Methods for Plasticity*. ISBN 9780470694527. doi:10.1002/9780470694626.

Fjaer, E., Holt, R.M., Horsrud, P., Raaen, A.M. and Risnes, R., 2008. *Petroleum related rock mechanics*, Vol. 53. Amsterdam, 2nd edition. ISBN 9780444502605.

Hasan, A.R. and Kabir, C.S., 2012. "Wellbore heat-transfer modeling and applications". doi:10.1016/j.petrol.2012.03.021.

Hasan, A. and Kabir, C., 1991. "Heat Transfer During Two-Phase Flow in Wellbores; Part I–Formation Temperature". pp. 469–478. doi:10.2118/22866-ms.

Jaeger, J.C., Cook, N. and Zimmerman, R., 2007. *Fundamentals of Rock Mechanics*. Backwell, 4th edition. ISBN 978-0632057597.

Kuhlman, K.L., 2013. "Review of inverse Laplace transform algorithms for Laplace-space numerical approaches". *Numerical Algorithms*, Vol. 63, No. 2, pp. 339–355. ISSN 10171398. doi:10.1007/s11075-012-9625-3.

Mendonça, P.d.T.R. and Fancello, E.A., 2019. *O método de Elementos Finitos aplicado à Mecânica dos Sólidos*. Orsa Maggiore. ISBN 978-85-907153-1-3.

Naumenko, K., 2006. *Modeling of High-Temperature Creep for Structural Analysis Applications*. Ph.D. thesis.

Oudeman, P. and Bacarreza, L.J., 1995. "Field Trial Results of Annular Pressure Behavior in a High-Pressure/High-Temperature Well". *SPE Drilling & Completion*.

Pattillo, P.D., Cocales, B.W. and Morey, S.C., 2006. "Analysis of an Annular Pressure Buildup Failure During Drill Ahead". *SPE Drilling & Completion*, Vol. 21, No. 04, pp. 242–247. ISSN 1064-6671. doi:10.2118/89775-pa.

Poiate Jr., E., Maia, A. and Falcao, J., 2006. "Well Design for Drilling Through Thick Evaporite Layers in Santos Basin—Brazil". In *Proceedings of IADC/SPE Drilling Conference*. Society of Petroleum Engineers, Miami, February. ISBN 978-1-55563-238-0. ISSN 19231555. doi:10.2523/99161-MS.

Taheri, S.R., Pak, A., Shad, S., Mehrgini, B. and Razifar, M., 2020. "Investigation of rock salt layer creep and its effects on casing collapse". *International Journal of Mining Science and Technology*. ISSN 20952686. doi:10.1016/j.ijmst.2020.02.001.

Wang, H.Y. and Samuel, R., 2016. "3D geomechanical modeling of salt-creep behavior on wellbore casing for presalt

reservoirs". *SPE Drilling and Completion*, Vol. 31, No. 4, pp. 261–272. ISSN 10646671. doi:10.2118/166144-PA.

Zhang, J., Standifird, W. and Lenamond, C., 2008. "Casing ultradeep, ultralong salt sections in deep water: A case study for failure diagnosis and risk mitigation in record-depth well". *Proceedings - SPE Annual Technical Conference and Exhibition*, Vol. 1, pp. 129–152. doi:10.2118/114273-ms.

7. RESPONSIBILITY NOTICE

The authors are solely responsible for the printed material included in this paper.